

# Exciton spin-flip rate in quantum dots determined by a modified local density of optical states

Jeppe Johansen, Brian Julsgaard, Søren Stobbe, Jørn M. Hvam, and Peter Lodahl\*  
DTU Fotonik, Department of Photonics Engineering,  
Technical University of Denmark, Ørsteds Plads 343, DK-2800 Kgs. Lyngby,  
Denmark. <http://www.fotonik.dtu.dk/quantumphotonics>

The spin-flip rate that couples dark and bright excitons in self-assembled quantum dots is obtained from time-resolved spontaneous emission measurements in a modified local density of optical states. Employing this technique, we can separate effects due to non-radiative recombination and unambiguously record the spin-flip rate. The dependence of the spin-flip rate on emission energy is compared in detail to a recent model from the literature, where the spin flip is due to the combined action of short-range exchange interaction and acoustic phonons. We furthermore observe a surprising enhancement of the spin-flip rate close to a semiconductor-air interface, which illustrates the important role of interfaces for quantum dot based nanophotonic structures. Our work is an important step towards a full understanding of the complex dynamics of quantum dots in nanophotonic structures, such as photonic crystals, and dark excitons are potentially useful for long-lived coherent storage applications.

PACS numbers: 78.67.Hc, 78.47.+p, 72.25.Fe

Understanding the optical properties of solid-state quantum emitters is much required due to their increasing importance for all-solid-state quantum photonic devices for quantum information processing [1]. Spin degrees of freedom of electrons and holes in semiconductor quantum dots (QDs) impose exciton fine structure: The long-lived *dark-exciton states* can recombine after a phonon-mediated spin-flip process, whereby a radiating bright exciton is formed [2, 3]. Dark exciton recombination is essential to explore: it influences the performance of QD single-photon sources [4, 5] and the quantum-optical properties of QDs [6], and must be accounted for when assessing inhibition of spontaneous emission in photonic crystals [7, 8]. Furthermore, long-lived spin states in the solid state are required for spin qubits [9], and dark excitons might be attractive in this context since they can be prepared and read out optically.

In a QD, the exciton spin lifetime is greatly extended compared to a bulk medium or a quantum well due to the discrete energy spectrum. The mechanism behind the spin-flip processes has been debated in the literature [10, 11], and experimental tests for unbiased QDs have been lacking. Here we employ controlled modifications of the local density of optical states (LDOS) to determine the dark exciton spin-flip rate from time-resolved spontaneous emission measurements. The LDOS is modified by placing QDs at controlled distances from a semiconductor-air interface, which was previously used to distinguish radiative and non-radiative recombination processes of bright excitons [12]. Controlling the LDOS provides a powerful tool to obtain detailed insight into QD dynamics; thus cavity quantum electrodynamics was recently employed for QD spectroscopy in the regime of continuous pumping [13]. We observe a surprising dependence of the spin-flip rate on the distance to the sample

surface ranging several hundred nanometers, and a sensitive dependence on the QD emission energy. The latter is compared in detail to theory describing the dependence of the spin-flip rate on QD size, and provides valuable insight on the exciton spin-flip mechanism in QDs.

Figure 1(a) illustrates the fine structure of the lowest exciton state for InAs/GaAs QDs [14]. The exciton is formed from the conduction band electron state (spin 1/2) and the heavy-hole valence band state (total angular momentum 3/2). As a result, four exciton states are formed. They are characterized by the projections of the total angular momentum onto the growth axis, which attain the values  $\pm 1$  or  $\pm 2$  for bright and dark excitons, respectively. The splitting between dark and bright energy levels  $\Delta_{db}$  is determined by the exchange coupling between electron and hole spins, and the bright-exciton levels are typically a few hundred  $\mu\text{eV}$  above the dark-exciton levels. The bright excitons  $|b\rangle$  decay to the ground state  $|g\rangle$  (no excitons) by emission of a photon through a dipole-allowed transition with a rate  $\gamma_{\text{rad}}$ . Radiative transitions from dark excitons  $|d\rangle$  are forbidden, however, they can decay through a phonon mediated spin-flip process (rate  $\gamma_{db}$ ) transforming the dark exciton into a bright exciton. The rate of the reverse process is denoted  $\gamma_{bd}$ . Finally non-radiative recombination was recently proven to be significant for self-assembled QDs [12], i.e., bright and dark excitons can recombine non-radiatively with rates denoted  $\gamma_{\text{nr}}^b$  and  $\gamma_{\text{nr}}^d$ , respectively.

We have measured spontaneous emission decay dynamics of InAs QDs positioned at 28 different distances from a GaAs/air interface, see inset of Fig. 1(b). Further experimental details can be found in Refs. [12, 15]. We record the number of photons emitted per time interval  $N(t)$  from the QDs. Solving the rate equations for the

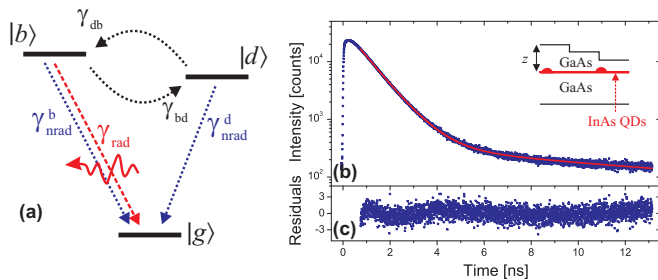


Figure 1: (Color online) (a) Three-level exciton scheme consisting of a bright  $|b\rangle$  and a dark  $|d\rangle$  state that are coupled through the spin-flip rates  $\gamma_{bd}$  and  $\gamma_{db}$ . Radiative recombination ( $\gamma_{rad}$ ) to the ground state  $|g\rangle$  (no exciton) is only possible for the bright state, while both the bright ( $\gamma_{nrad}^b$ ) and the dark state ( $\gamma_{nrad}^d$ ) can decay non-radiatively. (b) Typical decay curve acquired at a detection energy of 1.204 eV (blue squares) at the sample with QDs positioned 170 nm from the interface. The red line is a fit of the bi-exponential model to the data. **Inset** Sketch of the sample showing three different distances between the QDs and the GaAs-air interface. (c) The weighted residual obtained from the bi-exponential fit to the data resulting in  $\chi_R^2 = 1.11$ .

three-level system of Fig. 1(a) results in a bi-exponential decay  $N(t) = A_f e^{-\gamma_f t} + A_s e^{-\gamma_s t}$ . Here subscripts s and f denote slow and fast decay rates, respectively. Figure 1(b) shows an example of a spontaneous emission decay curve together with a bi-exponential fit obtained with a fixed background level to account for the measured contribution from dark-counts and after-pulsing of the detector. Excellent agreement between the experiment and the model is apparent from the weighted residuals reproduced in Fig. 1(c).

The four parameters  $\gamma_{f/s}$ ,  $A_{f/s}$  are obtained by fitting the experimental decay curves. We have  $\gamma_f \simeq \gamma_{rad} + \gamma_{nrad}^b$  and  $\gamma_s \simeq \gamma_{nrad}^d$ , where it has been assumed that the spin-flip rate is slow compared to both radiative and non-radiative processes, which is a very good approximation as seen below. Thus, the spin-flip rate cannot be obtained from the measured rates  $\gamma_{f/s}$  since they are dominated by other decay contributions. However, the amplitudes  $A_{f/s}$  contain additional information and the dark-bright spin-flip rate is contained in their ratio

$$\frac{A_f(z)}{A_s(z)} = \frac{\gamma_f(z) - \gamma_s}{\gamma_{db}(z)} \frac{\rho_b(t=0)}{\rho_d(t=0)} - 1, \quad (1)$$

where  $\rho_b(t=0)/\rho_d(t=0)$  is the ratio between the initial populations of bright and dark excitons after an excitation pulse and  $z$  is the distance to the interface. The repetitive nature of the experiment implies that the slow amplitude contains contributions from previous excitation pulses, which is accounted for by correcting the amplitudes according to  $A_s \rightarrow A_s (1 - e^{-\gamma_s T})$  where  $T = 13.5$  ns is the repetition period of the excitation laser. The spin-flip rate is obtained from experimentally

determined parameters by:

$$\gamma_{db}(z) = \frac{\gamma_f(z) - \gamma_s}{1 + A_f(z)/A_s(z)} \frac{\rho_b(t=0)}{\rho_d(t=0)}. \quad (2)$$

It is essential that the ratio of the amplitudes enters in Eq. (2) since the absolute size of  $A_{f/s}$  will depend on, e.g., the total collection efficiency of the radiated light or the number of QDs probed. Since the bright and dark excitons recombine radiatively on the same transition (cf. Fig. 1(a)) these dependencies do not contribute to the amplitude ratio. Quite remarkably, assessing the amplitudes allows for extraction of spin-flip rates that are slower than the repetition period of the measurement.

In Fig. 2 the slow decay rate and the ratio of the amplitudes are plotted versus distance to the interface. The fast rate (not shown) varies periodically with distance in full agreement with the modified LDOS caused by the reflecting interface [12]. In contrast, the slow decay rate is constant within the error-bars of the measurement, which confirms that it is dominated by non-radiative recombination of dark excitons ( $\gamma_{nrad}^d$ ). The average decay rate of  $\gamma_s = 0.097 \pm 0.008$  ns<sup>-1</sup> matches very well with the non-radiative decay rate of bright excitons at the same emission energy, which is expected since the bright and dark exciton binding energies are very close.  $A_f(z)/A_s(z)$  is expected to vary proportional to the LDOS through  $\gamma_f(z)$  (cf. Eq. (1)) and indeed clear oscillations with a period matching the LDOS is observed. In addition the spin-flip rate is found to vary, which gives rise to the overall increase of the amplitude ratio with  $z$ . Assuming an exponential decrease of the spin-flip rate with  $z$ , which will be discussed further below, and multiplying by the calculated LDOS we can model the experimental data very well, see Fig. 2(b).

In order to extract the spin-flip rate from Eq. (2), we need to estimate the ratio of the initial populations of bright and dark excitons. Due to the non-resonant excitation, the feeding of the QDs is non-geminate [16], thus dark and bright excitons are formed with equal probability. A slight imbalance between the initial populations is nonetheless created due to the finite probability of creating biexcitons. The recombination of biexcitons is dominated by radiative decay, which always leaves behind a bright exciton and thus increase  $\rho_b(0)$  relative to  $\rho_d(0)$ . The long lifetime of the dark excitons moreover increases the probability of biexciton formation since a residual population of dark excitons is persistent when the subsequent excitation re-excites the QDs. In the present experiment the excitation density was fixed such that on average 0.1 excitons were generated per QD and by solving the rate equations for the QD population including the biexciton level we find  $\rho_b(t=0)/\rho_d(t=0) \approx 1.25$ .

The spin-flip rate versus distance to the interface is presented in Fig. 3 for six different emission energies. It is found to vary between  $4.7 \mu\text{s}^{-1}$  and  $14.7 \mu\text{s}^{-1}$  corresponding to long-lived exciton spin lifetimes between 68 ns and

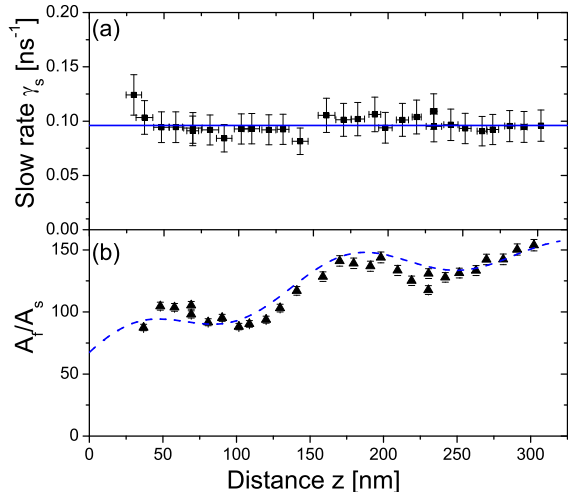


Figure 2: (Color online) (a) The slow decay rate as a function of distance to the interface measured at 1.204 eV. No systematic dependence on distance is observed confirming that the slow rate is due to non-radiative decay of dark excitons. The blue line indicates the averaged rate. (b) Measured ratio of the fast and slow amplitudes versus distance. The dashed blue curve is obtained by multiplying the calculated LDOS with an overall exponential decrease of the spin-flip rate with the distance to the interface.

215 ns. Surprisingly the spin-flip rate is observed to depend exponentially on distance to the interface, which is observed for all emission energies. The characteristic decay length varies between 24 nm and 106 nm. This increase of the spin-flip rate in the vicinity of the interface could be caused by enhancement of acoustic phonons at the interface. In this case, we estimate the phonon wavelength from  $\lambda_{\text{ph}} = hv/\Delta_{\text{db}}$  where  $h$  is Planck's constant,  $v$  is the sound speed and  $\Delta_{\text{db}}$  the exchange energy splitting between bright and dark states that must be matched by the phonons. For GaAs we estimate  $\lambda_{\text{ph}} \sim 65 - 85$  nm for longitudinal phonons using the range of exchange energies relevant in the experiment, which matches the length scale observed in the experiment.

The above results illustrate clearly the importance of nearby surfaces when seeking a quantitative understanding of the dynamics of QDs in nanostructures. Recent examples of intricate surface effects include the increased emission rate observed near a semiconductor interface [15], while charge trapping near surfaces was suggested as the mechanism responsible for the surprisingly large QD-nanocavity coupling efficiency at very large detunings observed under non-resonant excitation [17, 18, 19]. These are examples of the new physics found in solid-state implementations of quantum electrodynamics experiments.

Let us now consider the energy dependence of the spin-

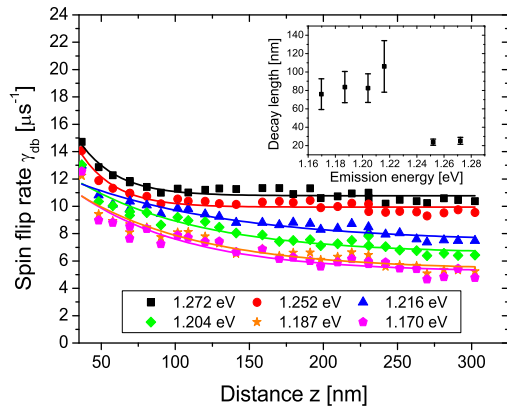


Figure 3: (Color online) The spin-flip rates versus distance  $z$  to the interface for six different emission energies. The plotted curves are fits to the experimental data assuming an exponential decay of the spin-flip rate with the distance to the interface. The inset shows the exponential decay length versus emission energy.

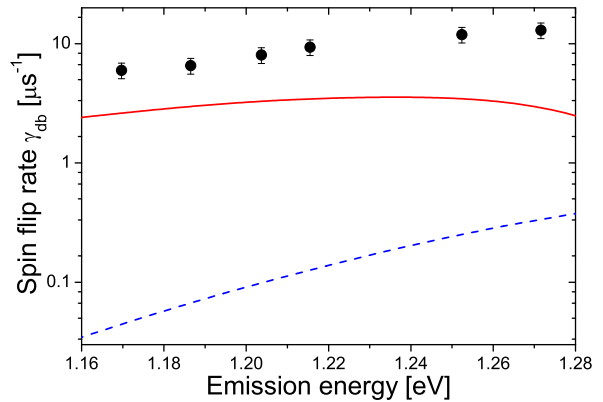


Figure 4: (Color online) Measured spin-flip rate at different emission energies for the sample with ( $z = 302$  nm) (solid black circles). The theoretically predicted spin-flip rate using the model of Ref. [10] for parameters that reproduce the energy dependence of the radiative decay rate (dashed blue line) and for optimized parameters (solid red line).

flip rate, which allows to assess how the spin-flip process varies with QD size. In order to minimize the effect of the interface, we plot in Fig. 4 the spin-flip rate versus energy for the sample with largest QD-interface distance ( $z = 302$  nm). The spin-flip rate is observed to increase significantly with the emission energy, and varies from  $6 \text{ ns}^{-1}$  at 1.170 eV to  $13 \text{ ns}^{-1}$  at 1.272 eV meaning that the characteristic spin-flip time can be prolonged by more than a factor of 2 by varying the QD size.

The energy-dependence of the spin-flip rate can be compared to theory using the model introduced in Ref. [10]. In this work the dark-bright exciton spin-flip rate was calculated due to the combined effect of short-range exchange interaction and acoustic phonons. A complex behavior is expected since the spin-flip rate is predicted to depend on the energy splitting between the lowest and first excited exciton states  $\Delta_{12}$ , the exchange energy splitting  $\Delta_{\text{db}}$ , as well as the size of the electron and hole wavefunctions.

The experimental data for the energy-dependent spin-flip rates are compared to theory using experimentally realistic parameters: By recording the emission spectrum of the QDs at high pump power where the ground state is saturated, we obtain  $\Delta_{12} = 120 \pm 20$  meV. The exchange splitting depends strongly on the indium mole fraction [20] and it is enhanced in QDs due to the strong localization of the electron and hole wavefunctions as described by the enhancement factor [21]. Furthermore, the spin-flip rate depends on the electron and hole wavefunctions through a form factor [22]. We have calculated the electron and hole wavefunctions using the theory and parameters of Ref. [15]. All other parameters are taken from Ref. [10] and the references given above.

The comparison to theory is presented in Fig. 4. The dashed blue curve is for parameters that reproduce the frequency dependence of the radiative decay rate [15] (aspect ratio: 1/2, indium mole fraction: 0.46, QD heights: between 4 nm and 5.8 nm). The observed increase of the spin-flip rate with energy is reproduced by the theory. However, the calculated rates are two orders of magnitude smaller than the measured values. We have explored the origin of this deviation by optimizing the model parameters in order to maximize the spin-flip rate, see the solid red curve in Fig. 4 (aspect ratio: 1/3, indium mole fraction: 0.90, QD heights: between 1.9 nm and 2.4 nm). In this case the predicted spin-flip rates approach the measured rates, although a systematic discrepancy is still observed. Furthermore, a rather weak frequency dependence of the spin-flip rate is predicted, since the finite confinement potentials impose lower limits to the achievable compression of the wavefunctions. We conclude that additional spin-flip processes must be included in a complete theory. Additional contributions may arise due to spin-orbit coupling [11] or long-range exchange effects [23].

In conclusion, we have measured the rate for spin flip from dark to bright excitons using time-resolved fluorescence spectroscopy. The spin-flip rate increases significantly when approaching the sample surface suggesting an enhancement due to surface acoustic phonons. The energy dependence of the spin-flip rate was compared to a recent theory, where the spin flip is induced by short-range exchange interaction between electrons and holes while the required energy is provided by acoustic phonons. Our results illustrate the importance of tak-

ing the QD fine structure into account when interpreting luminescence experiments, and will be important in order to obtain quantitative understanding of light-matter interaction in QD based optical devices.

We gratefully acknowledge the Danish Research Agency for financial support (projects FNU 272-05-0083, 272-06-0138 and FTP 274-07-0459).

---

\* Electronic address: pelo@fotonik.dtu.dk.

- [1] B. Lounis and M. Orrit, *Rep. Prog. Phys.* **68**, 1129 (2005).
- [2] O. Labeau, P. Tamarat, and B. Lounis, *Phys. Rev. Lett.* **90**, 257404 (2003).
- [3] J. M. Smith, P. A. Dalgarno, R. J. Warburton, A. O. Govorov, K. Karrai, B. D. Gerardot, and P. M. Petroff, *Phys. Rev. Lett.* **94**, 197402 (2005).
- [4] A. Strauf, N. G. Stoltz, M. T. Rakher, L. A. Coldren, P. M. Petroff, and D. Bouwmeester, *Nat. Photon.* **1**, 704 (2007).
- [5] T. Lund-Hansen, S. Stobbe, B. Julsgaard, H. Thyrrestrup, T. Sünner, M. Kamp, A. Forchel, and P. Lodahl, *Phys. Rev. Lett.* **101**, 113903 (2008).
- [6] M. Reischle, G. J. Beirne, R. Roßbach, M. Jetter, and P. Michler, *Phys. Rev. Lett.* **101**, 146402 (2008).
- [7] P. Lodahl, A.F. van Driel, I.S. Nikolaev, A. Irman, K. Overgaag, D. Vanmaekelbergh, and W.L. Vos, *Nature* **430**, 654 (2004).
- [8] B. Julsgaard, J. Johansen, S. Stobbe, T. Stolberg-Rohr, T. Sünner, M. Kamp, A. Forchel, and P. Lodahl, *Appl. Phys. Lett.* **93**, 094102 (2008).
- [9] A. Imamoğlu, D. D. Awschalom, G. Burkard, D. P. DiVincenzo, D. Loss, M. Sherwin, and A. Small, *Phys. Rev. Lett.* **83**, 4204 (1999).
- [10] K. Roszak, V. M. Axt, T. Kuhn, and P. Machnikowski, *Phys. Rev. B* **76**, 195324 (2007); erratum: *Phys. Rev. B* **77**, 249905(E) (2008).
- [11] E. Tsitsishvili, R. v. Baltz, and H. Kalt, *Phys. Rev. B* **72**, 155333 (2005).
- [12] J. Johansen, S. Stobbe, I. S. Nikolaev, T. Lund-Hansen, P. T. Kristensen, J. M. Hvam, W. L. Vos, and P. Lodahl, *Phys. Rev. B* **77**, 073303 (2008).
- [13] M. Winger, A. Badolato, K.J. Hennessy, E.L. Hu, and A. Imamoğlu, *Phys. Rev. Lett.* **101**, 226808 (2008).
- [14] M. Bayer, G. Ortner, O. Stern, A. Kuther, A. A. Gorbunov, A. Forchel, P. Hawrylak, S. Fafard, K. Hinzer, T. L. Reinecke, S. N. Walck, J. P. Reithmaier, F. Klopff, and F. Schäfer, *Phys. Rev. B* **65**, 195315 (2002).
- [15] S. Stobbe, J. Johansen, P.T. Kristensen, J.M. Hvam, and P. Lodahl, submitted, cond-mat arXiv:0902.0344v1 (2009).
- [16] B. Baylac, X. Marie, T. Amand, M. Brousseau, J. Barreau, and Y. Shekun, *Surface Science* **326**, 161 (1995).
- [17] K. Hennessy, A. Badolato, M. Winger, D. Gerace, M. Atatüre, S. Gulde, S. Fält, E. L. Hu, and A. Imamoğlu, *Nature (London)* **445**, 896 (2007).
- [18] M. Kaniber, A. Laucht, A. Neumann, J. M. Villas-Bôas, M. Bichler, M.-C. Amann, and J. J. Finley, *Phys. Rev. B* **77**, 161303(R) (2008).
- [19] A. Laucht, F. Hofbauer, N. Hauke, J. Angele, S. Stobbe,

- M. Kaniber, G. Böhm, P. Lodahl, M.-C. Amann, and J.J. Finley, *New Journ. of Physics* **11**, 023034 (2009).
- [20] H. Fu, L.-W. Wang and A. Zunger, *Phys. Rev. B.* **59**, 5568 (1999).
- [21] R. Romestain and G. Fishman, *Phys. Rev. B* **49**, 1774 (1994).
- [22] A. Grodecka, L. Jacak, P. Machnikowski, and K. Roszak, in "Quantum Dots: Research Developments", edited by P. A. Ling (Nova Science, New York, 2005); arXiv:cond-mat/0404364.
- [23] J.W. Luo, A. Franceschetti and A. Zunger, *Phys. Rev. B* **79**, 201301(R) (2009).